ORIGINAL ARTICLE

Application of metal cored filler wire for environmental-friendly welding of low alloy steel: experimental investigation and parametric optimization

Kumar Abhishek[1] · Vishalkumar Prajapati[1] · Soni Kumari[2] · Balaji Krushna Potnuru[3] · Din Bandhu[4]

Abstract

Motivated by the crescente demand for eco-friendly and worker-safe welding techniques, this study optimizes current (A), voltage (V), and gas flow rate (GFR) for regulated metal deposition (RMD) welding of ASME SA387 Gr.11 Cl.2 steel. Employing MEGAFIL 237 M metal cored filler wire and a Taguchi L_9 orthogonal array, bead-on-plate trials were conducted to evaluate heat-affected zone (HAZ), depth of penetration (DOP), and bead width (BW). A unique dual-pronged optimization approach was implemented. The utility function method, combined with Taguchi's signal-to-noise (S/N) ratio, maximized desirable and minimized undesirable responses. Additionally, TOPSIS with Taguchi S/N ratio identified the optimal process parameters. Both optimization strategies converged on identical. A = 135 A, V = 14 V, and GFR = 13 L/min. Notably, voltage emerged as the most influential factor in the mean S/N response table, highlighting its critical role in controlling weld quality. The proposed procedures offer a robust framework for determining optimal RMD welding conditions in pipeline applications. This not only enhances weld integrity and worker safety but also paves the way for sustainable manufacturing and continuous quality improvement in the field.

Keywords RMD welding · Weld bead geometry · Low alloy steel · TOPSIS · Utility function · Taguchi method

1 Introduction

Technology advancement in today's fast-paced world compels nearly all factories and engineering companies to produce long-lasting, high-quality goods at competitive prices. While many products are created independently as standalone pieces, they often need to be put together in order to function in their intended real-world contexts [1–4]. Welding is the method of choice in several sectors (including the automotive, aviation, hydrocarbon, pharmaceutical, power, and agricultural industries) for joining thick and thin, and often incompatible materials to easily produce efficient, durable, and cost-effective products [5–8]. Welding saves time and money when compared to other methods like adhesive bonding and mechanical fastening of joining materials. It creates a weld so strong and durable that it's nearly impossible to detach the joined pieces. The American Welding Society (AWS) recognizes 94 distinct welding methods, one of which is gas metal arc welding (GMAW) [9–11].

GMAW has been employed in a broad range of industries since its commercialization in the late 1950s, including shipyards, gasoline and oil pipelines, pressure vessels, boiler pipes, heat exchangers, coal conversion, and chemical parts. There are three ways in which metal can be transferred: globular arc transfer, spray arc transfer, and shortcircuiting arc transfer. Out of these three modes of metal transfer, the shortcircuiting mode of metal transfer is quite popular

✉ Din Bandhu
din.bandhu@manipal.edu

1 Department of Mechanical and Aerospace Engineering, Institute of Infrastructure, Technology, Research and Management (IITRAM), Ahmedabad, Gujarat 380026, India

2 Department of Mechanical Engineering, GLA University, Mathura, U.P 281406, India

3 Department of Mechanical Engineering, Malla Reddy Engineering College (Autonomous), Hyderabad, Telangana 500100, India

4 Department of Mechanical and Industrial Engineering, Manipal Institute of Technology Bengaluru, Manipal Academy of Higher Education, Manipal, Karnataka 576104, India

due to its attributes like versatility in welding metals of different thicknesses and out-of-position welding capability. Although the short-circuiting method of metal transfer has its benefits, it also has certain downsides. In turn, it produces localized arc heat, which slows down the pace of the deposition process. When welding thick plates (6.35 mm or higher), cold lapping or a lack of fusion might develop if the best procedure is not used. When the machinery isn't optimized properly, excessive spatter results from incorrect short-circuiting, which causes the unit to overheat [12–14].

To address the aforementioned issues, Miller Electric Mfg. LLC developed a revolutionary welding approach that improves on the conventional shortcircuiting mode of the GMAW technique. The manufacturer named this novel technique "regulated metal deposition" (RMD) due to its nature of controlling and adjusting the welding arc precisely with respect to the base material [15–17]. The company claims that this advanced method employs a sophisticated welding current waveform to control the short circuit. The thickness and constitution of the metal being joined are two factors that frequently affect waveform. As may be seen in Fig. 1, it can be broken down into seven separate stages. Each of these seven stages contributes to a larger cycle known as the RMD cycle [18]. Detailed explanations of the RMD cycle's individual stages can be found in Fig. 2.

The "ball" stage of an RMD cycle is characterized by a spike in current that melts the electrode head and results in a short circuit. The current drops off during the subsequent "background" stage, permitting the short circuit to take place. The "pre-short" stage then follows, during which the current is lowered to a safe level to shield the steady weld puddle from the arc force. When the molten head is in contact with the base metal at a lower current, this is known as the "wet" stage. The "pinch" stage involves a quick rise in current at the electrode head, producing the "pinch effect," and resulting in a short circuit. The pinch effect is observed during the transitional period between the "pinch" and "clear" stages. As the "clear" stage concludes, the molten head separates from the electrode. The "blink" stage, in which short circuits are broken and the current significantly declines, closes the circuit and ends the cycle [19–21].

Numerous scholars have suggested using GMAW and/or GTAW methods for welding low-alloy steel. Nevertheless, there are constraints inherent to these methods. On one side, GMAW is fast but unable to produce spatter-free and slag-free welds; on the other hand, GTAW produces spatter-free and slag-free welds but has the limitation of slow welding speed. Therefore, these conventional welding approaches are not financially sustainable in the current production context. This means that improvements in welding technology are essential. Take a look at the characteristics of RMD welding (in Table 1), which is as quick as GMAW and creates spatter- and slag-free welds like GTAW [22–24].

Quality is a top priority in today's production perspective. Quality is the extent to which a product satisfies its intended consumer. The product's quality is determined by
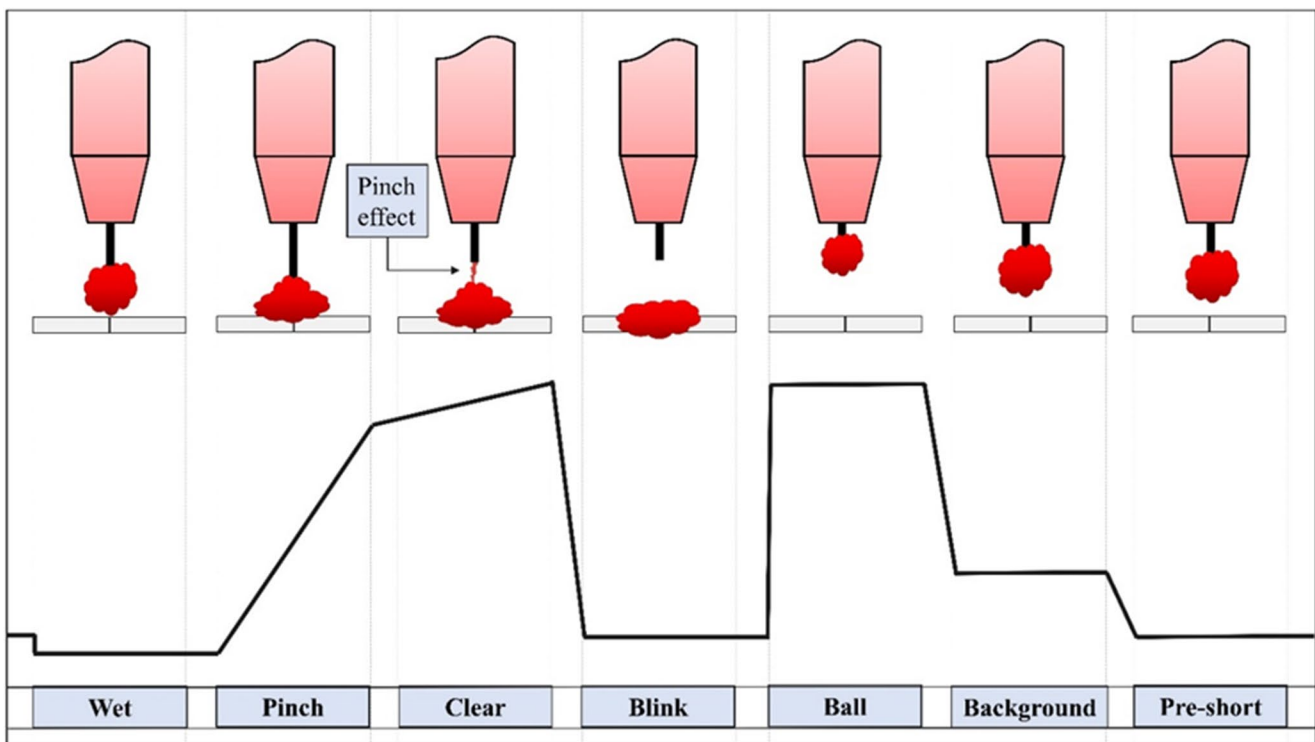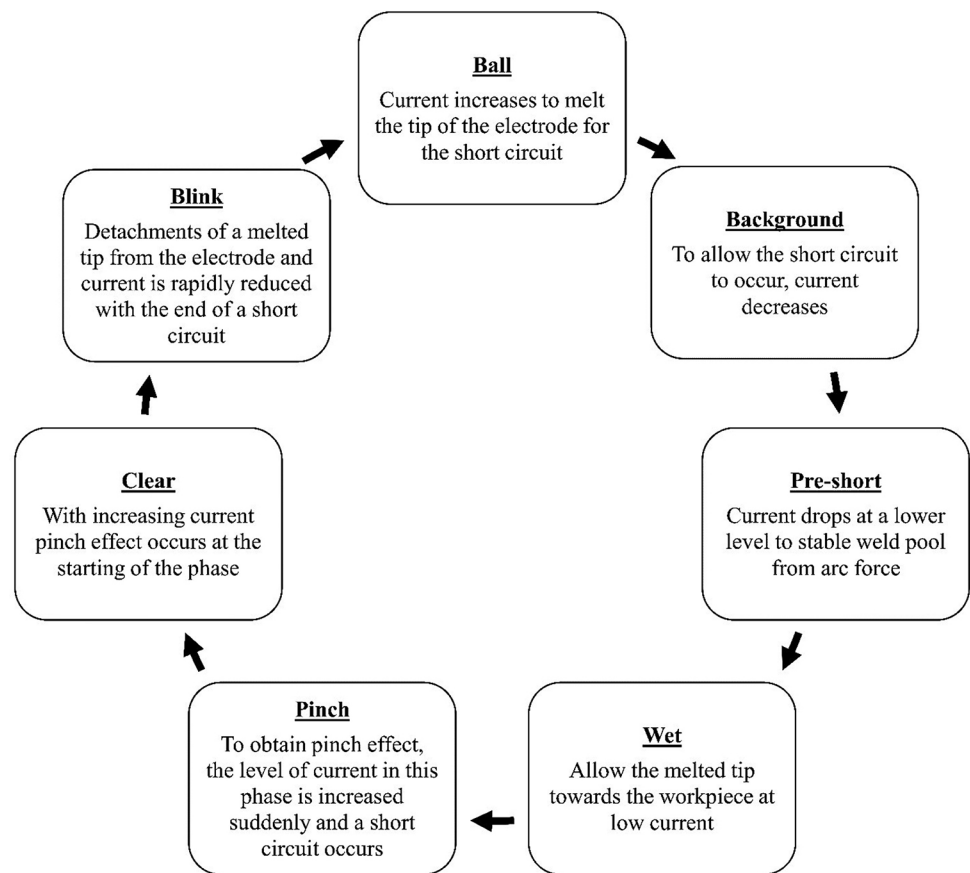

Fig. 1 Different stages of metal transfer in the RMD process [18]

Fig. 2 The RMD cycle

Table 1 Comparative advantages of the RMD technique over conventional arc welding processes

Attributes	RMD	GMAW	GTAW
Travel speeds (in./min)	6–12	6–10	3–5
Training time required	Less	Moderate	More
Spatter and slag generation	No	Yes	No
Post-weld re-work required	No	Yes	Seldom
Repositioning of pipes (starts and stops)	Seldom	Often	Often

how well it meets the needs of its intended purpose in a variety of contexts [25–27]. Weld quality in the welding industry is primarily determined by the mechanical behavior of the weldments, which are in turn controlled by their chemical and metallurgical compositions. Weld bead geometry (WBG), which is closely connected to welding variables, also affects the mechanical-metallurgical aspects of the weldment. To summarize, welding variables determine weld quality. In the metalworking industry, arc welding techniques are widely recognized as among the most versatile and effective. A complicated interaction between a number of process variables affects the weld chemistry, mechanical characteristics, and metallurgical aspects of the weld joint, as well as the WBG. As a result, it is important to identify the best welding process conditions for achieving the specified weld quality. On the other hand, the optimization

should be carried out in such a manner that all objectives are met concurrently. This type of optimization approach is known as multi-response optimization [28–33].

According to the available publications, several researchers have spent time perfecting techniques for modeling, simulating, and optimizing traditional arc welding procedures. To determine welding variables resulting in an ideal approach, a comprehensive study has been performed to identify correlations between welding variables, WBG, weld quality, and productivity [34–37]. WBG during electric arc welding was studied by Mistry [38], who looked at how different welding factors impacted the process. The effects of the input factors V, A, W_S, and base metal-electrode tip distance on the resulting BW, DOP, and BH were analyzed. The research recommends using full penetration for the most robust and cost-effective welds. Furthermore, the research suggests that currently has a significant impact on penetration whereas voltage affects BW. RMD welding on low-carbon steel pipes was carried out by Costa and Vilarinho [39]. Tests have been conducted while the input variables of wire feed speed (W_{FS}), W_S, trim (T_M), arc control, and weaving are all considered. No intrinsic defects like porosity, absence of fusion, or cracking were found during analysis. After conducting a macroscopic analysis of the specimens, it was discovered that raising the W_{FS} led to an improvement in

penetration and root reinforcement (R_R) and a drop in face reinforcement (R_F). The T_M has also been the subject of research. WBG grows in tandem with the T_M. This results in a reduction of R_F. This study by Nouri et al. [40] analyzed the effect of pulsed-GMAW factors on the WBG. W_S, W_{FS}, vertical angle, and nozzle-to-workpiece distance were selected as the main factors. The degree to which they had an effect was determined by analyzing the WBG produced. Improvements in W_{FS} are associated with improvements in BH, BW, and DOP, whereas decreases in these responses are seen with increments in W_S. GMAW and RMD welding were used by Das et al. [41] to join 10 mm thick 2.25 Cr-1.0 Mo grade steel. Electrodes made of metal-cored wire were utilized as the filler. Samples were heat-treated after welding so that any resulting microstructural changes could be studied. The welded joints were also put through mechanical testing, with favorable findings. Joints with a root misalignment (High/Low) of 1.5 mm can be produced using either traditional or enhanced short-circuit GMAW procedures, as determined by a comparison of both techniques by Vilarinho and Nascimento [16]. Although updated GMAW welding procedures produced more durable components, traditional welding techniques produced weaker welds. To predict the WBG while accumulating 316 L stainless steel onto structural steel IS2062, Murugan et al. [42] created mathematical equations employing a five-level factorial method. OCV, W_{FS}, W_S, and nozzle-to-plate distance have all been studied for their effects on the responses of dilution, reinforcement, penetration, and width. The accuracy and practicality of the proposed modeling techniques have been verified. In order to aid in the choosing of process variables to obtain the required level of the overlay, graphical representations of the primary and interaction impacts of the control variables on dilution and WBG have been shown. Submerged arc welding (SAW) was performed on high-strength low-alloy steel by Sharma et al. [43] to examine the impact of various input variables on the final WBG. The WBG during cooling was observed as a function of the input factors of heat input and preheat temperatures. To demonstrate the relationship between preheating temperature and cooling time, a mathematical model was developed using the response surface method. Artificial neural networks (ANN) and genetic algorithms (GA) were utilized by Nagesh and Dutta [43] to investigate the WBG and provide the optimal result for GTAW. The "multiple layer regression" technique was utilized to create mathematical models, which took into account both the impacts of the input variables and the two-factor interactions. The effect of SAW elements on WBG was studied by Choudhary et al. [44]. Welding current, OCV and nozzle-to-plate distance were the input factors. BW, reinforcement, and penetration were the process's results. In the investigation, it was shown that

a higher current resulted in more reinforcement and penetration. To optimize the voltage, current, welding speed, and arc length in arc welding for rail car bracket assembly, Daniyan et al. [44] used the Taguchi approach and response surface methods (RSM). Taguchi analysis was used to assess how well the process performed in terms of hardness and distortion, and RSM was employed to analyze how the various input components interacted with one another. The researchers also published the results of an analysis of variance (ANOVA) and a regression analysis of the empirical study in order to assess the efficacy of the suggested model. Additional notable applications of optimization approaches in welding have been described by Vora et al. [45]. Datta et al. [46]. Dhas and Dhas [47], Karpagaraj et al. [48]. Benyounis and Olabi [49], and Chen et al. [50]. , .

Based on the research published so far, it is evident that a lot of effort has been put into assessing the HAZ, DOP, and BW properties of conventional arc welding methods. Welding factors such as V, A, GFR, etc. have been optimized using a variety of methods throughout the process. Researchers haven't even tried much with more sophisticated GMAW methods like RMD welding. Machine specifications and the RMD process's applicability are the sole topics covered in the manufacturer's literature. However, no experimental evidence is discussed. As a result, there is a dearth of cutting-edge information about RMD welding. Therefore, the purpose of this research is to evaluate the WBG of low alloy steel and provide a novel optimization approach by employing utility function and TOPSIS approaches, both of which are important additions to the existing academic database covering this cutting-edge welding technique.

2 Materials and methods

RMD bead-on-plate (BOP) welding was carried out on a Cr-Mo Gr. 11 Cl. 2 (500 mm x 150 mm x 06 mm) steel plate with the assistance of semi-automatic welding equipment (Miller's continuous 500). In everyday conversation, chromium-molybdenum steel is referred to as 1 ¼ chrome, although its official designation in the industry is either ASME SA387 or ASTM A387. Cr-Mo Gr. 11 Cl. 2 is applicable in many industries and general purposes such as the oil & gas industry, petrochemical industry, boilers & heat exchangers, shipping, automobile ancillaries, steel plants; cement industry, sugar industry, nuclear & aerospace pants, centrifugal industry, steel plants, port building, wastewater management, paper & pulp industry, and infrastructure building. It is useful in raising temperatures because it can handle high temperatures. It has higher flexibility, durability, longevity, good dimensional accuracy, weldability, excellent surface finishing, higher tensile strength,

Table 2 Chemical composition of ASME SA387–Gr.11–Cl.2 steel and MEGAFIL 237 M

Element	Chromium (Cr)	Molybdenum (Mo)	Carbon (C)	Manganese (Mn)	Phosphorus (P)	Sulfur (S)	Silicon (Si)
Base metal (Content %)	1.00–1.50	0.45–0.65	0.05–0.17	0.40–0.65	0.035	0.035	0.50
Wire electrode (Content %)	2.3	1.1	0.07	1.0	0.015	0.015	0.3

Table 3 Continuum 500 welding machine's specifications

Type of input power supply	3Φ
Voltage range	10–44 V
Current range	20–600 A
Maximum OCV (Open Circuit Voltage)	75 V
Rated welding output	500 amps @ 40 load volts; 100% Duty cycle

sturdiness, and can withstand heavy loads. These plates can entirely stress cracking corrosion resistance, crevice corrosion resistance, and pitting resistance [45–47].

The choice of consumables like filler material has a significant impact on both efficient and cost-effective manufacturing and the emission of harmful gases throughout the process. As filler materials, fabricators typically employ solid filler wire (SFW), flux-cored filler wire (FCFW), and metal-cored filler wire (MCFW) during arc welding operations. The MCFWs are the most recent addition to the welding world and offer the most advantages in terms of performance, profitability, and sustainability [48, 49]. Incorporating features from both the SFW and FCFW, MCFWs provide a unique set of advantages. They combine the rapid deposition rates of an FCFW with the streamlined operation of an SFW. When comparing deposition rates, a 1.2 mm MCFW and a 1.6 mm MCFW are superior to both an SFW and an FCFW [48]. MCFW has quicker travel speeds,

greater duty factor, decreased mill scale difficulties, slag-free and spatter-free weld formation, lessened weld flaws like porosity, lack of fusion, and undercut, and eliminates cleaning and post-weld activities like grinding [50, 51]. Due to these features, a 1.2 mm thick metal-cored 'MEGAFIL 237 M' wire was used as the wire electrode. The elements of the ASME SA387—Gr. 11—Cl. 2 steel as well as the wire electrode are presented in Table 2. As a shielding gas, 90% argon and 10% carbon dioxide have been combined. The specs of the welding machine are presented in Table 3, and Fig. 3 illustrates how the machine should be configured for the study.

Adjustments made to the welding variables have a substantial impact on the dynamic properties of GMAW. In terms of voltage, current, shielding gas, the diameter of filler metal, feeder speed, and gas flow rate, these kinds of adjustments can take place. Current (A), voltage (V), and gas flow rate (L/min) were taken into account as the governing variables for the study based on the accessibility and configuration of the welding equipment. Table 4 displays the variations that were made to these variables at three distinct levels.

When preparing and analyzing experimental studies, the design of experiments (DOE) is an essential tool. Since the experimental studies are so time- and resource-intensive, establishments are unable to conduct the trials at all available variable settings and evaluate the optimal potential
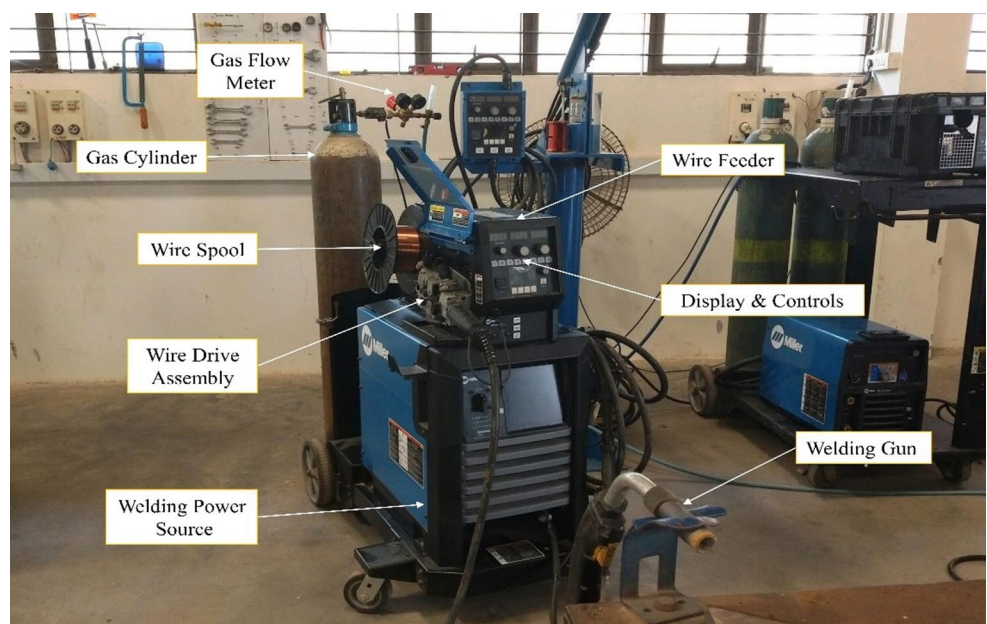
Fig. 3 Miller's Continuum 500 welding machine

Table 4 Parameters and their levels

Governing variables	Level (L)		
	1	2	3
A	125	135	145
V	14	16	18
GFR	13	16	19

Table 5 Experimental sets based on Taguchi's L_9 OA

Trial No.	A	V	GFR
1.	125	14	13
2.	125	16	16
3.	125	18	19
4.	135	14	16
5.	135	16	19
6.	135	18	13
7.	145	14	19
8.	145	16	13
9.	145	18	16

findings [52–57]. Because of this, the importance of DOE cannot be overstated. Some of the DOE methods with their benefits and drawbacks are shown in Fig. 4 [58–62].

Taguchi's orthogonal array (OA) idea is used here because of its many practical advantages. It's a simple concept that performs well in a wide range of industrial contexts, thereby making it an adaptable yet uncomplicated method. It improves process or product quality by concentrating on the mean value of an output attribute that is close to the goal value rather than on the value within defined limitations. And despite the fractional nature of the approach, it guarantees parity across all levels of all variables [57, 63–66]. In light of this, the experimental sets (Table 5) have been arranged according to Taguchi's L_9 OA.

Nine bead-on-plate (BOP) experiments were carried out as per the aforementioned experimental sets utilizing a Continuum 500 welding machine at a steady speed of 8.85 inches per minute (ipm). Figure 5 contains a presentation of the BOP experiments that were conducted.

Once the plates had cooled, they were sliced to 30 mm x 10 mm (as shown in Fig. 6) using a MAXMEN band saw machine. The output characteristics, including DOP, HAZ, and BW, were measured by inspecting the cut specimens underneath a microscope after they had been polished, etched, and hydrated with water. Figure 7 depicts the measurement terminology for all nine specimens, and Table 6 lists the measured responses.

3 Result and discussion

This section discusses the applied approaches and their outcomes for obtaining the best welding input variables for WBG during RMD welding of ASME SA387 Gr.11 Cl.2 steel. In this context, two statistical optimization techniques
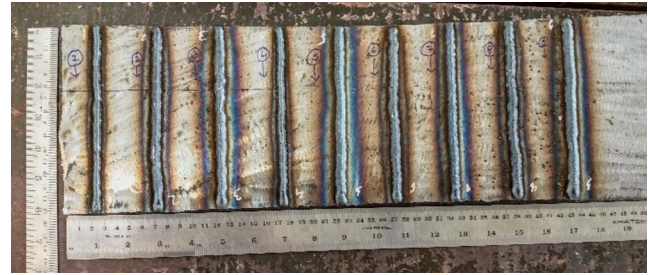
Fig. 5 BOP trials on ASME SA387 Gr.11 Cl.2 steel plates

Fig. 6 Sample preparation for Macroscopy

namely Utility and TOPSIS have been explored with Taguchi Method.

3.1 Utility function approach

Utility functions are a commonly accepted concept in multi-criteria decision-making (MCDM) problems due to their simplicity and ease of understanding for decision-makers. They do not require any additional constraints beyond

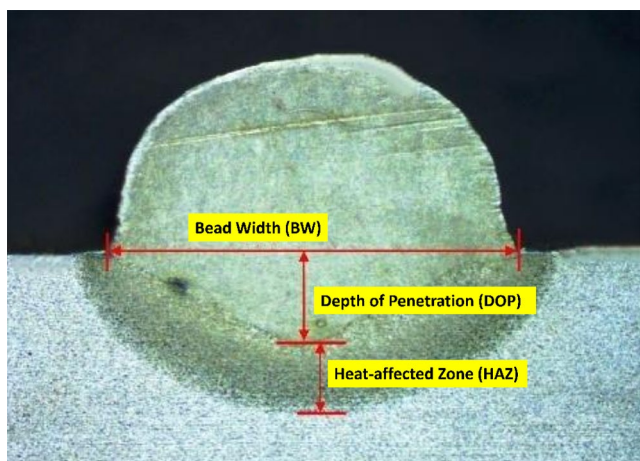**Fig. 4** General DOE techniques used in engineering applications [58–62]

Increasing accuracy →

Decreasing cost ↓

Full Factorial Array
If cost is not a big issue (having enough time, runs are inexpensive), or the accuracy is critical

Taguchi Orthogonal Array
If cost is high (having limited/no time, runs are expensive), or the accuracy is not so critical

Taguchi Non-Orthogonal Array
If cost is prohibitive (runs are extremely time consuming or expensive), and limited accuracy is acceptable

Fig. 7 Measurement terminology of output responses

Table 6 Measured output responses

Trial No.	HAZ	DOP	BW
	All dimensions are in 'mm'		
1.	1.100	1.300	5.920
2.	1.910	1.538	7.450
3.	1.980	1.404	7.340
4.	1.260	1.278	5.720
5.	1.860	1.396	7.470
6.	1.740	2.117	7.750
7.	1.510	1.476	7.200
8.	1.770	1.293	6.820
9.	2.510	1.625	8.850

the aggregation formula. In the utility-based Taguchi process, an MCDM problem can be transformed into a single response optimization problem using a response function, also known as an arbitrary function, which acts as an overall utility index. The goal is to optimize this function to obtain the solution [67–69]. According to the utility function approach [70], if A_x is the performance indicator of an output response x and there are k output characteristics evaluating the data set, the joint utility function can be expressed as follows:

$$U\left(A_1, A_2, \ldots \ldots A_k\right) = f\left\{U_1\left(A_1\right), U_2\left(A_2\right), \ldots \ldots U_k\left(A_k\right)\right\} \qquad (1)$$

In Eq. (1), the utility of the x_{th} output response is represented by $(U_1(A_1))$. Equation (2) shows the overall utility function, which is equal to the sum of the utilities of individual output characteristics.

$$U\left(A_1, A_2, \ldots \ldots A_k\right) = \sum_{x=1}^{k} U_x(A_x) \qquad (2)$$

The weightage given to the output responses is based on their relative importance and impact on the process. In

this case, the overall utility function can be understood as follows:

$$U\left(A_1, A_2, \ldots \ldots A_k\right) = \sum_{x=1}^{k} W_x U_x(A_x) \qquad (3)$$

In Eq. (3), W_x represents the importance or influence assigned to the output response x. The total of all the weights assigned to all the output responses should be 1. The output values are evaluated based on lower and higher values using two random arithmetic values 0 and 9 (preference numbers) as benchmarks. Equation (4) can be used to evaluate the preference number N_p on a logarithmic scale.

$$N_p = O * \log\frac{A_x}{A'_x} \qquad (4)$$

In Eq. (4), A_x represents the value of output characteristic x. A'_x is the lower value of output characteristic x. O is a constant and can be calculated using Eq. (5), only if $A_x = A^*$ (where A^* is the optimal value), then $N_p = 9$. Hence

The value of output response x is represented by A_x in Eq. (4). The lower value of output response x is represented by A'_x. O is a constant that can be found using Eq. (5) if A_x is equal to the optimal value, denoted as A^*. If this is the case, then N_p is equal to 9. Therefore,

$$O = \frac{9}{\log\frac{A_x}{A'_x}} \qquad (5)$$

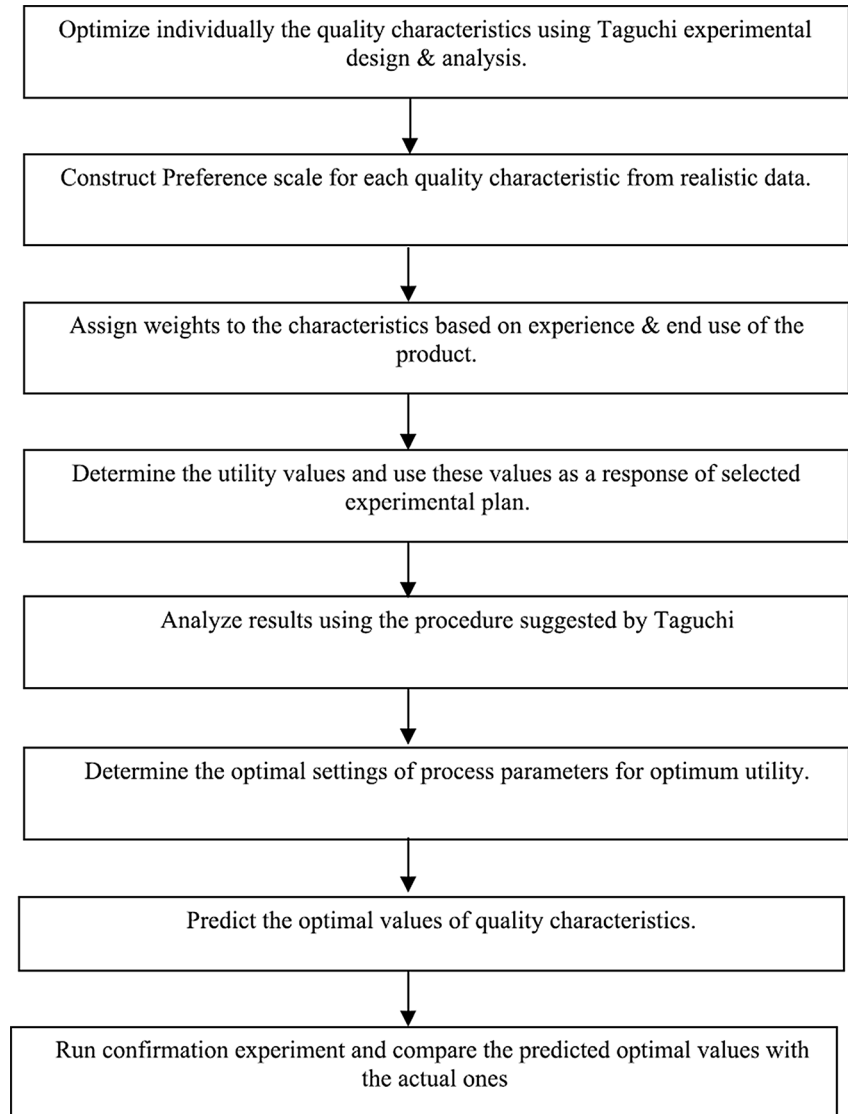The utility in its whole is expressed as:

$$U = \sum_{x=1}^{k} W_x(N_p) \qquad (6)$$

Under the condition:

$$\sum_{x=1}^{k} W_x = 1 \qquad (7)$$

The S/N ratio concept developed by Taguchi involves three different output characteristics: nominal-is-best (NB), lower-is-better (LB), and higher-is-better (HB). Among these, HB is relevant for evaluating utility functions. Therefore, when maximizing the utility function, the output attributes considered in the assessment process will be automatically optimized, either by being minimized or maximized, depending on the specific situation. The optimization method used is illustrated in Fig. 8.

A series of experiments were conducted using the L_9 orthogonal array and the resulting responses, including

Fig. 8 The flow path of the Utility Taguchi approach

Optimize individually the quality characteristics using Taguchi experimental design & analysis.

Construct Preference scale for each quality characteristic from realistic data.

Assign weights to the characteristics based on experience & end use of the product.

Determine the utility values and use these values as a response of selected experimental plan.

Analyze results using the procedure suggested by Taguchi

Determine the optimal settings of process parameters for optimum utility.

Predict the optimal values of quality characteristics.

Run confirmation experiment and compare the predicted optimal values with the actual ones

Table 7 S/N ratio and predicted S/N ratio for overall utility

U1	U2	U3	$U_{overall}$	SNRA2	PSNRA2
9.000	0.277	8.291	5.856	15.35195	18.36375
2.980	3.299	3.551	3.277	10.30846	
2.588	1.598	3.858	2.681	8.566765	
7.518	0.000	9.000	5.506	14.81698	
3.270	1.598	3.496	2.788	8.905653	
3.997	9.000	2.737	5.245	14.39442	
5.544	2.590	4.255	4.129	12.3179	
3.811	0.139	5.373	3.107	9.848206	
0.000	4.312	0.000	1.437	3.150487	

HAZ, DOP, and BW, were recorded and presented in Table 6. Since these responses conflicted with each other, it was necessary to convert them to a common scale. In this context, the utility function approach was used to combine all the conflicting criteria into a single index called the overall utility. First, the individual utility for each of the responses was

determined using Eqs. 4 and 5. For HAZ and BW, lower values were preferable, while a higher value was desired for DOP. As shown in Table 7, all of these responses were converted to a scale ranging from 0 to 9, with 0 representing the lowest utility value and 9 representing the highest. By using Eq. 6, it was then possible to combine all of these responses into a single overall utility index, which is also presented in Table 7. The Taguchi S/N ratio was then applied to the overall utility to find the optimal welding condition. From Fig. 9, it was determined that the optimal welding condition is a current of 135 A, a voltage of 14 V, and a gas flow rate of 13 L/min. Additionally, Table 8 shows that voltage is the variable that has the greatest impact on the results.

3.2 TOPSIS method

The TOPSIS method, short for Technique for Order Preference by Similarity to Ideal Solution, is a multi-attribute
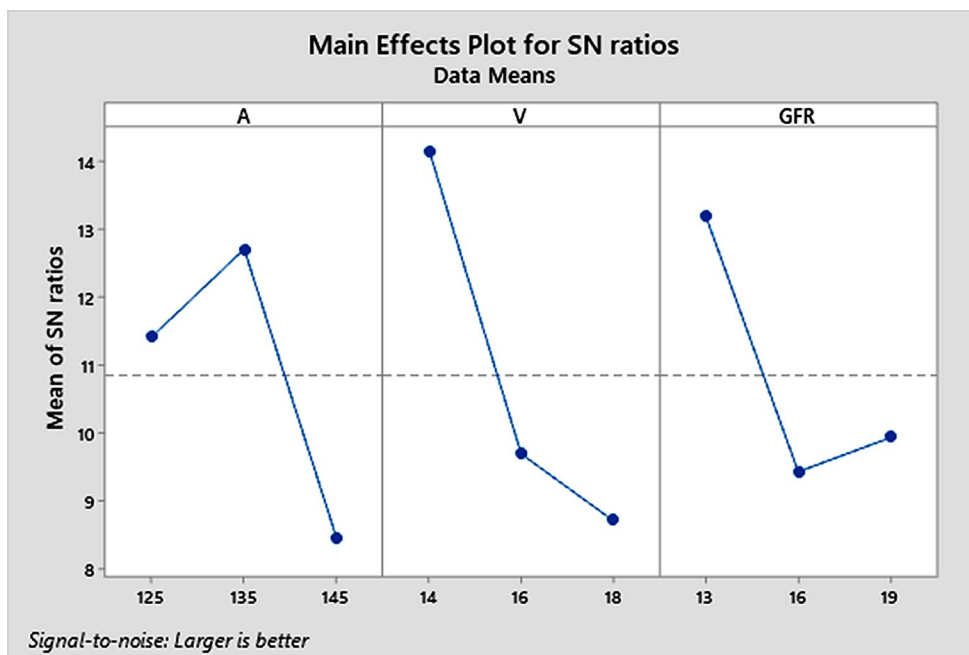
Fig. 9 Main effect plot for U$_{overall}$

Table 8 S/N ratios mean response table

Level	A	V	GFR
1	11.409	14.162	13.198
2	12.706	9.687	9.425
3	8.439	8.704	9.93
Delta	4.267	5.458	3.773
Rank	2	1	3

decision-making technique used to identify the best options for solving a problem within a solution space. It was introduced in 1981 by Ching-Lai Hwang and Kwangsun Yoon and is known for its simplicity and ease of understanding and implementation [71–73]. The method involves evaluating the degree of proximity to the ideal solution, which should be as close as possible to the positive ideal solution (made up of the best performance values among all options) and as far as possible from the negative ideal solution (made up of the worst performance values) [73–75]. TOPSIS has a wide range of applications, including engineering and design, logistics, marketing, manufacturing, and supply chain management, and it is straightforward to program and use, with a consistent number of steps regardless of the problem size [76, 77]. The method involves converting multiple attributes into a single response through a series of following steps [74]:

Step 1 Creating a decision matrix:

$$D = \begin{array}{c} A_1 \\ A_2 \\ . \\ A_i \\ . \\ A_m \end{array} \begin{bmatrix} x_{11} & x_{12} & . & x_{1j} & x_{1n} \\ x_{21} & x_{22} & . & x_{2j} & x_{2n} \\ . & . & . & . & . \\ x_{i1} & x_{i2} & . & x_{ij} & . \\ . & . & . & . & . \\ x_{m1} & x_{m2} & . & x_{mj} & x_{mn} \end{bmatrix} \quad (8)$$

A_i (where i ranges from 1 to m) represents the potential replacements, and x_j (where j ranges from 1 to n) represents the characteristics that relate to the substitute's performance. The performance of A_i for attribute $X_{j.}$ is represented by x_{ij}.

Step 2 Decision matrix normalization;

$$r_{ij} = \frac{x_{ij}}{\sqrt{\sum_{i=1}^{m} x_{ij}^2}} \quad (9)$$

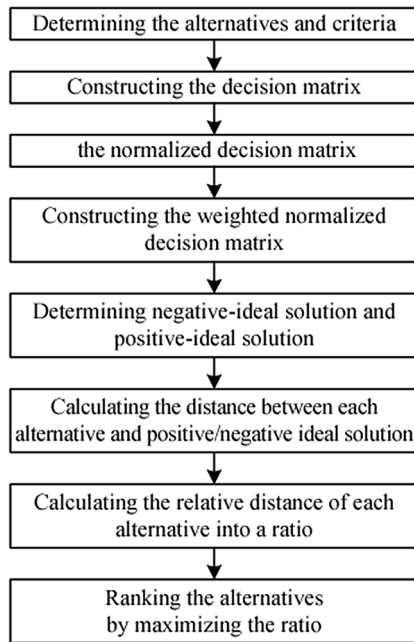r_{ij} represents the performance of A_i normalized for attribute $X_{j.}$

Fig. 10 TOPSIS method's flow path

Step 3 Assigning weightage to the normalized decision matrix:

$$D = \begin{bmatrix} y_{11} & y_{12} & \cdot & y_{1j} & y_{1n} \\ y_{21} & y_{22} & \cdot & y_{2j} & y_{2n} \\ \cdot & \cdot & \cdot & \cdot & \cdot \\ y_{i1} & y_{i2} & \cdot & y_{ij} & \cdot \\ \cdot & \cdot & \cdot & \cdot & \cdot \\ y_{m1} & y_{m2} & \cdot & y_{mj} & y_{mn} \end{bmatrix} \quad (10)$$

$$V = [v_{ij}] \ V = w_j r_{ij}$$

where, $\sum_{j=1}^{n} w_j = 1$

Step 4 Identifying the most favorable (positive best) and least favorable (negative worst) solutions.

a) Most favorable solution:
$$A^+ = \left\{ \left(\max_i y_{ij} \,|\, j \in J \right), \left(\min_i y_{ij} \,|\, j \in J' \,|\, i = 1,2,\ldots\ldots,m \right) \right\}$$
$$= \left\{ y_1^+, y_2^+, \ldots\ldots\ldots, y_j^+, \ldots\ldots y_n^+ \right\} \quad (11)$$

b) Least favorable solution:
$$A^- = \left\{ \left(\min_i y_{ij} \,|\, j \in J \right), \left(\max_i y_{ij} \,|\, j \in J' \,|\, i = 1,2,\ldots\ldots,m \right) \right\}$$
$$= \left\{ y_1^-, y_2^-, \ldots\ldots\ldots, y_j^-, \ldots\ldots y_n^- \right\} \quad (12)$$

where,
$$J = \{ j = 1,2,3,\ldots\ldots\ldots, n \,|\, j \} : \text{beneficial features}$$

Table 9 Experimental data for normalization and assigned weightage

N-HAZ	N-DOP	N-BW	W-HAZ	W-DOP	W-BW
0.206	0.286	0.273	0.068	0.097	0.090
0.357	0.339	0.344	0.118	0.115	0.113
0.370	0.308	0.339	0.122	0.105	0.112
0.236	0.282	0.264	0.078	0.096	0.087
0.348	0.308	0.345	0.115	0.105	0.114
0.326	0.467	0.358	0.107	0.159	0.118
0.283	0.326	0.332	0.093	0.111	0.110
0.331	0.284	0.315	0.109	0.097	0.104
0.470	0.359	0.408	0.155	0.122	0.135

Table 10 Most favorable (positive best) and least favorable (negative worst) solutions

	HAZ	DOP	BW
A-	0.155	0.096	0.135
A+	0.068	0.159	0.087

$$J' = \{ j = 1,2,3,\ldots\ldots\ldots, n \,|\, j \} : \quad \text{nonbeneficial}$$
features

Step 5 Measuring the distance between substitutes and the ideal solution. The distance between each substitute and the ideal solution is determined using n-dimensional Euclidean distance calculations using these equations.

$$S_i^+ = \sqrt{\sum_{j=1}^{n} \left(y_{ij} - y_j^+ \right)^2} \, i = 1,2,\ldots\ldots\ldots, m \quad (13)$$

$$S_i^- = \sqrt{\sum_{j=1}^{n} \left(y_{ij} - y_j^- \right)^2} \, i = 1,2,\ldots\ldots\ldots, m \quad (14)$$

Step 6 Evaluation of the overall performance coefficient nearest to the ideal solution.

$$C_i^+ = \frac{S_i^-}{S_i^+ + S_i^-}, i = 1,2,\ldots\ldots\ldots, m; 0 \leq C_i^+ \leq 1 \quad (15)$$

A flow diagram of the optimization process used in this study is shown in Fig. 10.

The experiments were conducted using the L_9 orthogonal array, and the results (HAZ, DOP, and BW) were recorded and presented in Table 9. The results were then normalized using Eq. 9 and the normalized values are shown in Table 9. In this study, all of the responses were given equal importance, so equal weightage was assigned to each response using Eq. 10 (shown in Table 9). Since the responses are conflicting, it is necessary to determine the most favorable and least favorable solutions (shown in Table 10) using Eqs. 11 and 12, respectively. In this context, lower values for HAZ and BW were preferred, so the lowest values for these responses were considered the most favorable solutions and

vice versa. Similarly, higher values for DOP were preferred, so the highest value for DOP was considered the most favorable solution and vice versa. The separation distance from the positive and negative ideal solutions was then calculated using Eqs. 13 and 14, respectively, and listed in Table 11. The closeness coefficient was then determined using Eq. 15, with the highest value being the preferred result. Finally, the Taguchi method of S/N ratio was applied to the closeness coefficient to determine the optimal welding combination, which was found to be a current of 135 A, a voltage of 14 V, and a gas flow rate of 13 L/min (shown in Fig. 11). The predicted S/N ratio was also calculated to validate the optimal combination, and it was observed from Table 11 that the predicted S/N ratio was higher than the other computed S/N ratios, supporting the chosen optimal combination. The mean response table in Table 12 shows that voltage is the most significant governing variable.

4 Conclusions

This study evaluates and optimizes current, voltage, and gas flow rate for regulated metal deposition (RMD) welding on ASME SA387 Gr. 11 Cl. 2 steel in terms of the heat-affected zone (HAZ), depth of penetration (DOP), and bead width (BW). The following conclusions are derived:

i.   Using a dual-pronged optimization approach (Utility-Taguchi and TOPSIS with Taguchi S/N ratio), this study identified the optimal welding parameters as 135 A current, 14 V voltage, and 13 L/min gas flow rate.

Table 11 The separation distance from the most favorable (positive best) and least favorable (negative worst) solutions together with closeness coefficient and S/N ratios

S+	S-	C+	SNRA1	PSNRA1
0.0618	0.0980	0.613	-4.24584	-1.18307
0.0714	0.0470	0.397	-8.02477	
0.0806	0.0411	0.338	-9.42624	
0.0639	0.0909	0.587	-4.62744	
0.0765	0.0463	0.377	-8.4715	
0.0502	0.0805	0.616	-4.20627	
0.0589	0.0684	0.537	-5.39756	
0.0767	0.0553	0.419	-7.55582	
0.1059	0.0260	0.197	-14.0967	

Table 12 S/N ratios mean response table

Level	A	V	GFR
1	-7.232	-4.757	-5.336
2	-5.768	-8.017	-8.916
3	-9.017	-9.243	-7.765
Delta	3.248	4.486	3.58
Rank	3	1	2

ii. Analysis of the S/N ratio revealed voltage as the most influential factor, highlighting its critical role in controlling HAZ, DOP, and bead width.

iii. The established methods offer a reliable framework for determining optimal RMD welding conditions in various applications.

iv. Implementing these optimized parameters can enhance welding integrity, and worker safety, and pave the way for sustainable manufacturing and continuous quality improvement in pipeline welding across various industries.

Fig. 11 Main effects plot for parametric settings
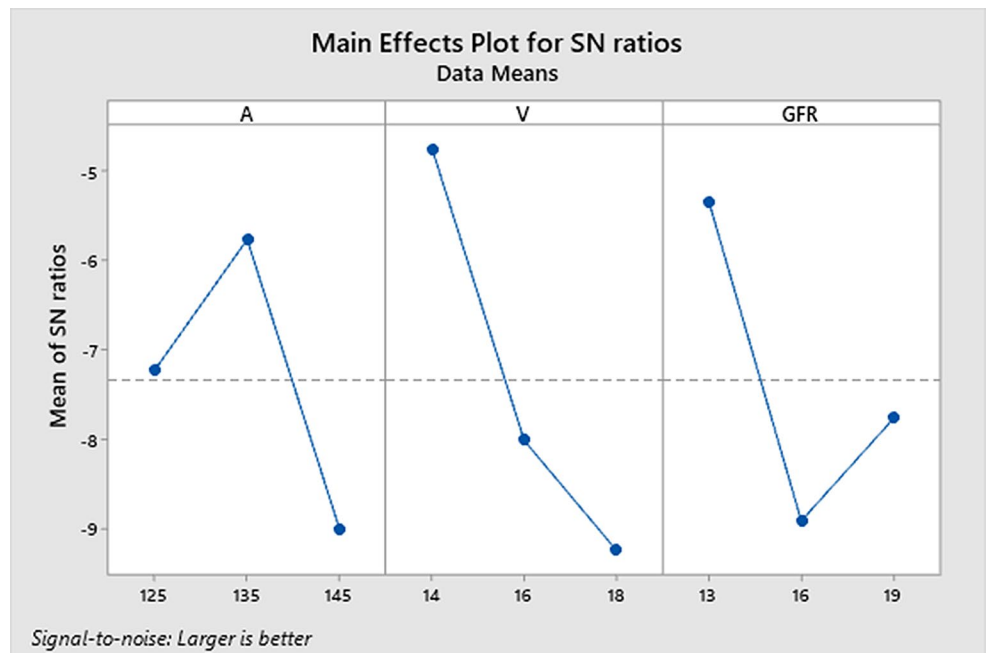
The work may further be extended by investigating the applicability of these optimization methods to other steel grades and material types beyond ASME SA387 Gr.11 Cl.2. Development and validation of predictive models and simulations can further optimize RMD welding settings and exploring the relationship between process parameters and microstructure/mechanical properties.

Declarations

Conflict of interest The authors have no known financial or personal affiliations that might have impacted this work.

References

1. Murtha, T.P., Lenway, S.A., Hart, J.A.: Managing New Industry Creation: Global Knowledge Formation and Entrepreneurship in High Technology.~(book review). (2001)
2. Bandhu, D.: Experimental Investigation and Parametric Optimization of Regulated Metal Deposition Welding for Low Alloy Steel, /articles/(2021). https://doi.org/10.6084/M9.FIGSHARE.19161509.V1
3. Adin, M., Okumuş, M.: Investigation of Microstructural and Mechanical properties of Dissimilar Metal Weld between AISI 420 and AISI 1018 STEELS. Arab. J. Sci. Eng. **47**, 8341–8350 (2022). https://doi.org/10.1007/s13369-021-06243-w
4. Jha, P., Shaikshavali, G., Shankar, M.G., Ram, M.D.S., Bandhu, D., Saxena, K.K., Buddhi, D., Agrawal, M.K.: A hybrid ensemble learning model for evaluating the Surface Roughness of AZ91 Alloy during the end milling operation. Surf. Rev. Lett. (2022). https://doi.org/10.1142/S0218625X23400012
5. Bandhu, D., Jani, S., Thakur, A.: Characterization of Frictional stir Welding for two dissimilar materials and influence of Ageing on their Mechanical Properties. Int. J. Res. Eng. IT Soc. Sci. **07**, 21–25 (2017)
6. Bandhu, D., Kumar, R., Nishant, A., Thakur, A.: Characterization of Friction Stir Welding for AA 2014–6061 and influence of Aging on their Mechanical Behavior. In: 5th National Conference on Topical Transcend in Mechanical Technology SJBIT Bangalore (TTMT-17). pp. 98–102 (2017)
7. Adin;, H., Doğan, A., Adin, M.: Examination of the Weld defects in the Inner-City Natural Gas Pipes with non-destructive and destructive testing methods. J. Sci. Technol. Eng. Res. **2**, 46–57 (2021). https://doi.org/10.5281/zenodo.4755095
8. Muchhadiya, A., Kumari, S., Bandhu, D., Abhishek, K., Vora, J.J.: Elucidating the Effect of Friction stir Welding variables on HDPE sheets using Grey Integrated with fuzzy: Experimental investigation and Parametric Optimization. JOM 2023. 1–9 (2023). https://doi.org/10.1007/S11837-023-05839-X
9. Bandhu, D., Kumari, S., Prajapati, V., Saxena, K.K., Abhishek, K.: Experimental investigation and optimization of RMDTM welding parameters for ASTM A387 grade 11 steel. Mater. Manuf. Process. **36**, 1524–1534 (2021). https://doi.org/10.1080/10426914.2020.1854472
10. Bandhu, D., Goud, E.V., Vora, J.J., Das, S., Abhishek, K., Gupta, R.K., Thakur, A., Kumari, S., Devi, K.D.: Influence of Regulated Metal Deposition and Gas Metal Arc Welding on ASTM A387-11-2 Steel plates: As-deposited inspection, microstructure, and Mechanical properties. J. Mater. Eng. Perform. 1–14 (2022). https://doi.org/10.1007/s11665-022-07185-6
11. Kumari, S., Bandhu, D., Muchhadiya, A., Abhishek, K.: Recent trends in parametric influence and microstructural analysis of friction stir welding for polymer composites, https://www.tandfonline.com/doi/abs/10.1080/2374068X.2023.2193447, (2023). https://doi.org/10.1080/2374068X.2023.2193447
12. Miller Welds: Guidelines For Gas Metal Arc Welding (GMAW), (2018). millerwelds.com/-/media/miller-electric/files/pdf/resources/mig_handbook.pdf
13. Dinbandhu, Prajapati, V., Vora, J.J., Das, S., Abhishek, K.: Experimental studies of Regulated Metal Deposition (RMD™) on ASTM A387 (11) steel: Study of parametric influence and welding performance optimization. J. Brazilian Soc. Mech. Sci. Eng. **42**, 1–21 (2020). https://doi.org/10.1007/s40430-019-2155-3
14. Kah, P., Suoranta, R., Martikainen, J.: Advanced gas metal arc welding processes. Int. J. Adv. Manuf. Technol. **67**, 655–674 (2013). https://doi.org/10.1007/s00170-012-4513-5
15. Cuhel, J., Packard, K.: RMD® Short-Circuit Metal Transfer, Pulsed MIG Processes with Metal-Cored. Wires Improve Pipe Fabrication for Swartfager Welding, Inc. (2009)
16. Das, S., Vora, J.J., Patel, V.: Regulated metal deposition (RMD™) technique for Welding applications: An Advanced Gas Metal Arc Welding process. In: Advances in Welding Technologies for Process Development, pp. 23–32. CRC (2019). https://doi.org/10.1201/9781351234825-2
17. Dinbandhu, Prajapati, V., Vora, J.J., Abhishek, K.: Advances in gas metal arc welding process: modifications in short-circuiting transfer mode. In: Advanced Welding and Deforming. pp. 67–104. Elsevier (2021). https://doi.org/10.1016/b978-0-12-822049-8.00003-7
18. Prajapati, V., Dinbandhu, Vora, J.J., Das, S., Abhishek, K.: Study of parametric influence and welding performance optimization during regulated metal deposition (RMD™) using grey integrated with fuzzy taguchi approach. J. Manuf. Process. **54**, 286–300 (2020). https://doi.org/10.1016/j.jmapro.2020.03.017
19. Miller Welds: New MIG Technology Makes Welders Immediately Productive On Stainless Steel Root Pass: (2018).
20. Cuhel, J., Benson, D.: Welding Stainless Steel Tube and Pipe. Maintaining Corrosion Resistance and Increasing Productivity (2009)
21. Roth, M.: Graham Corporation Meets Reduced Rework Objectives With Help from Miller's PipeWorx™ Welding Systems, (2009)
22. Miller Welds: RMD and Pulsed MIG Processes with Metal-Cored Wires Improve Pipe Fabrication for Swartfager Welding, Inc. 1–5 (2018)
23. Norrish, J., Cuiuri, D.: The controlled short circuit GMAW process: A tutorial. J. Manuf. Process. **16**, 86–92 (2014). https://doi.org/10.1016/j.jmapro.2013.08.006
24. Bandhu, D., Abhishek, K.: Assessment of Weld bead geometry in modified shortcircuiting gas metal arc welding process for low

alloy steel. Mater. Manuf. Process. **36**, 1384–1402 (2021). https://doi.org/10.1080/10426914.2021.1906897

25. Dinbandhu, Thakur, A., Venugopal Goud, E., Abhishek, K., Vora, J.J.: An overview of Proteus: The World's First Man-made non-cuttable material. In: Lecture Notes in Mechanical Engineering, pp. 95–102. Springer, Singapore (2021). https://doi.org/10.1007/978-981-16-3033-0_9

26. Tripathi, D.R., Vachhani, K.H., Bandhu, D., Kumari, S., Kumar, V.R., Abhishek, K.: Experimental investigation and optimization of abrasive waterjet machining parameters for GFRP composites using metaphor-less algorithms. Mater. Manuf. Process. **36**, 803–813 (2021). https://doi.org/10.1080/10426914.2020.1866193

27. Gajera, H., Djavanroodi, F., Kumari, S., Abhishek, K., Bandhu, D., Saxena, K.K., Ebrahimi, M., Prakash, C., Buddhi, D.: Optimization of Selective Laser Melting Parameter for Invar Material by Using JAYA Algorithm: Comparison with TLBO, GA and JAYA. Mater Vol 15, Page 8092. 15, 8092 (2022). (2022). https://doi.org/10.3390/MA15228092

28. Datta, S., Bandyopadhyay, A., Pal, P.K.: Grey-based taguchi method for optimization of bead geometry in submerged arc bead-on-plate welding. Int. J. Adv. Manuf. Technol. **39**, 1136–1143 (2008). https://doi.org/10.1007/s00170-007-1283-6

29. Bousnina, K., Hamza, A., Ben Yahia, N.: An integration of PSO-ANN and ANFIS hybrid models to predict surface quality, cost, and energy (QCE) during milling of alloy 2017A. J. Eng. Res. (2023). https://doi.org/10.1016/J.JER.2023.09.016

30. Bousnina, K., Hamza, A., Ben Yahia, N.: Predictive optimization of surface quality, cost, and energy consumption during milling alloy 2017A: An approach integrating GA-ANN and RSM models. Int. J. Interact. Des. Manuf. 1–20 (2023). https://doi.org/10.1007/S12008-023-01613-0/TABLES/13

31. Bousnina, K., Hamza, A., Ben Yahia, N.: An energy survey to optimize the technological parameters during the milling of AISI 304L steel using the RSM, ANN, and genetic algorithm. Adv. Mater. Process. Technol. (2023). https://doi.org/10.1080/2374068X.2023.2253658

32. Bousnina, K., Hamza, A., Ben Yahia, N.: A combination of PSO-ANN hybrid algorithm and genetic algorithm to optimize technological parameters during milling 2017A alloy. J. Ind. Prod. Eng. **40**, 554–571 (2023). https://doi.org/10.1080/21681015.2023.2243312

33. Bandhu, D., Djavanroodi, F., Shaikshavali, G., Vora, J.J., Abhishek, K., Thakur, A., Kumari, S., Saxena, K.K., Ebrahimi, M., Attarilar, S.: Effect of metal-cored Filler Wire on Surface morphology and micro-hardness of regulated metal deposition welded ASTM A387-Gr.11-Cl.2. Steel Plates Mater. 2022. **15**, 15, 6661 (2022). Page 6661 https://doi.org/10.3390/MA15196661

34. Chong, E.K.P., Zak, S.H.: An introduction to optimization. IEEE Antennas Propag. Mag. **38**, 60 (1996). https://doi.org/10.1109/MAP.1996.500234

35. Diwekar, U.M., Boston, M.A.: https://doi.org/10.1007/978-1-4757-3745-5. (2003)

36. Chatterjee, S., Mahapatra, S.S., Lamberti, L., Pruncu, C.I.: Prediction of welding responses using AI approach: Adaptive neuro-fuzzy inference system and genetic programming. J. Brazilian Soc. Mech. Sci. Eng. 2022 442. **44**, 1–15 (2022). https://doi.org/10.1007/S40430-021-03294-W

37. Bandhu, D., Vora, J.J., Das, S., Thakur, A., Kumari, S., Abhishek, K., Sastry, M.N.: Experimental study on application of gas metal arc welding based regulated metal deposition technique for low alloy steel. Mater. Manuf. Process. **37**, 1–19 (2022). https://doi.org/10.1080/10426914.2022.2049298

38. Mistry, J.P.: Effect of process parameters on bead geometry and shape relationship of Gas Metal Arc Weldments. Int. J. Adv. Res. Mech. Eng. Technol. **2**, 24–27 (2016)

39. Costa, T.F., Vilarinho, L.O.: Influence of Process Parameters During the Pipe Welding of Low-Carbon Steel Using RMD (Regulated Metal Deposition) Process. In: Proceedings of COBEM ; 21st Brazilian Congress of Mechanical Engineering Copyright © 2011 by ABCM October 24–28, 2011, Natal, RN, Brazil. pp. 1–10 (2011). (2011)

40. Nouri, M., Abdollah-Zadeh, A., Malek, F.: Effect of welding parameters on dilution and weld bead geometry in cladding. J. Mater. Sci. Technol. **23**, 817–822 (2007)

41. Das, S., Vora, J.J., Patel, V., Li, W., Andersson, J., Pimenov, D.Y., Giasin, K., Wojciechowski, S.: Experimental investigation on welding of 2.25 Cr-1.0 Mo steel with regulated metal deposition and GMAW technique incorporating metal-cored wires. J. Mater. Res. Technol. **15**, 1007–1016 (2021). https://doi.org/10.1016/j.jmrt.2021.08.081

42. Murugan, N., Parmar, R.S., Sud, S.K.: Effect of submerged arc process variables on dilution and bead geometry in single wire surfacing. J. Mater. Process. Technol. **37**, 767–780 (1993). https://doi.org/10.1016/0924-0136(93)90135-S

43. Sharma, S.K., Maheshwari, S., Singh, R.K.R.: Effect of heat-input and cooling-time on bead characteristics in SAW. Mater. Manuf. Process. **34**, 208–215 (2019). https://doi.org/10.1080/10426914.2018.1532578

44. Choudhary, D.K., Jindal, S., Mehta, N.P.: To study the effect of welding parameters on weld bead geometry in SAW welding process. Elixir Mech. Engg. **40**, 5519–5524 (2011). https://doi.org/10.4236/jmmce.2011.109064

45. Yadav, G.P.K., Bandhu, D., Krishna, B.V., Gupta, N., Jha, P., Vora, J.J., Mishra, S., Saxena, K.K., Salem, K.H., Abdullaev, S.S.: Exploring the potential of metal-cored filler wire in gas metal arc welding for ASME SA387-Gr.11-Cl.2 steel joints. J. Adhes. Sci. Technol. 1–22 (2023). https://doi.org/10.1080/01694243.2023.2223367

46. Adin, M.: A parametric study on the mechanical properties of MIG and TIG welded dissimilar steel joints. J. Adhes. Sci. Technol. (2023). https://doi.org/10.1080/01694243.2023.2221391

47. ADİN, M.: Lazer Kaynağı Ile Kaynak Yapılan Alüminyum Alaşımlarının Mekanik Özelliklerinin Araştırılması ve Kaynak Parametrelerinin Taguchi ve ANOVA Yöntemleri Kullanılarak Optimizasyonu. J. Sci. Technol. Eng. Res. **3**, 50–59 (2022). https://doi.org/10.53525/JSTER.1174394

48. Welding Engineers: Metal Cored Wires vs Solid Wire, https://weldingengineers.co.nz/news/welding-assistance/metal-cored-wires-vs-solid-wire

49. Miller Welds: Solid Wire Versus Flux-Cored Wire: When to Use Them and Why, https://www.millerwelds.com/resources/article-library/solid-wire-versus-flux-cored-wire-when-to-use-them-and-why, last accessed 2021/06/16

50. Hobart Filler Metals: Know the Basics to Get the Best Results from Metal-Cored Wire, https://www.hobartbrothers.com/news/178/523/Know-the-Basics-to-Get-the-Best-Results-from-Metal-Cored-Wire.html

51. Barhorst, S.: Understanding metal-cored wire, https://www.thefabricator.com/article/arcwelding/understanding-metal-cored-wire

52. Rajput, C., Kumari, S., Prajapati, V., Dinbandhu, Abhishek, K.: Experimental investigation on peel strength during ultrasonic welding of polypropylene H110MA. In: Materials Today: Proceedings. pp. 1302–1305. Elsevier (2020). https://doi.org/10.1016/j.matpr.2020.02.259

53. Tripathi, D.R., Vachhani, K.H., Kumari, S., Dinbandhu, Abhishek,, K.: Experimental investigation on material removal rate during abrasive water jet machining of GFRP composites. Mater. Today Proc. **26**, 1389–1392 (2020). https://doi.org/10.1016/j.matpr.2020.02.280

54. Murali Mohan, M., Venugopal Goud, E., Deva Kumar, M.L.S., Kumar, V., Kumar, M., Dinbandhu: Parametric Optimization

and Evaluation of Machining Performance for Aluminium-based hybrid composite using utility-Taguchi Approach. In: Lecture Notes in Mechanical Engineering, pp. 289–300. Springer, Singapore (2021). https://doi.org/10.1007/978-981-16-3033-0_27

55. ADİN, M., İŞCAN, B.: BADAY, Ş.: Taguchi Yöntemi Kullanılarak Sürtünme Kaynağı Ile Birleştirilen AISI 431 ve AISI 1020 Bağlantılarının Kaynak Parametrelerinin Optimizasyonu. Bilecik Şeyh Edebali Üniversitesi Fen Bilim Derg. (2022). https://doi.org/10.35193/bseufbd.1075980

56. ADİN, M.: Performances of cryo-treated and untreated cutting tools in machining of AA7075 aerospace aluminium alloy. Eur. Mech. Sci. **7**, 70–81 (2023). https://doi.org/10.26701/EMS.1270937

57. ADİN, M., İŞCAN, B.: Optimization of process parameters of medium carbon steel joints joined by MIG welding using Taguchi method. Eur. Mech. Sci. **6**, 17–26 (2022)

58. Olakanmi, E.O.: Optimization of the quality characteristics of laser-assisted Cold-Sprayed (LACS) Aluminum Coatings with Taguchi Design of experiments (DOE). Mater. Manuf. Process. **31**, 1490–1499 (2016). https://doi.org/10.1080/10426914.2014.984306

59. Rahang, M., Patowari, P.K.: Parametric Optimization for Selective Surface Modification in EDM using Taguchi Analysis. Mater. Manuf. Process. **31**, 422–431 (2016). https://doi.org/10.1080/10426914.2015.1037921

60. Ridzuan, N., Adam, F., Yaacob, Z.: Screening of factor influencing wax deposition using full factorial experimental design. Pet. Sci. Technol. **34**, 84–90 (2016). https://doi.org/10.1080/10916466.2015.1122625

61. Rakić, T., Kasagić-Vujanović, I., Jovanović, M., Jančić-Stojanović, B., Ivanović, D.: Comparison of full Factorial Design, Central Composite Design, and Box-Behnken Design in Chromatographic Method Development for the determination of Fluconazole and its impurities. Anal. Lett. **47**, 1334–1347 (2014). https://doi.org/10.1080/00032719.2013.867503

62. Adin, M.: Optimization of mechanical properties of composites obtained from textile wastes using Taguchi and ANOVA methods. (2022)

63. Taiwo, A.E., Madzimbamuto, T.N., Ojumu, T.V.: Optimization of process variables for acetoin production in a bioreactor using Taguchi orthogonal array design. Heliyon. **6**, e05103 (2020). https://doi.org/10.1016/j.heliyon.2020.e05103

64. Vinayak, H., Baghini, M.S., Apte, P.: Design and optimization of high precision CMOS voltage reference using Taguchi orthogonal array technique. In: 2011 International Symposium on Integrated Circuits, ISIC 2011. pp. 575–578 (2011). https://doi.org/10.1109/ISICir.2011.6131928

65. Kansal, S., Verma, A.S., Kant, S., Pankaj, N.A.: Parametric study of sisal-epoxy resin composite treated in sodium bicarbonate solution using Taguchi orthogonal array. Int. J. Mater. Eng. Innov. **11**, 264 (2020). https://doi.org/10.1504/ijmatei.2020.108886

66. Adin, M.: Investigation of optimum friction welding parameters and energy consumption for Ramor 500 and AISI 420 steels. (2022)

67. Pavan, M., Todeschini, R.: Multicriteria Decision-Making Methods. In: Comprehensive Chemometrics. pp. 591–629. Elsevier (2009). https://doi.org/10.1016/B978-044452701-1.00038-7

68. Bagada, C., Damor, H., Prajapati, V., Abhishek, K.: Utility Function Approach Integrated with fuzzy for optimization in Milling Glass Fiber Reinforced Epoxy composites. In: Recent Advances in Mechanical Infrastructure, pp. 85–91. Springer, Singapore (2020). https://doi.org/10.1007/978-981-32-9971-9_10

69. Kumari, S., Bandhu, D., Kumar, A., Yadav, R.K., Vivekananda, K.: Application of utility function Approach aggregated with Imperialist competitive algorithm for optimization of turning parameters of AISI D2 Steel. In: Recent Advances in Mechanical Infrastructure, pp. 49–57. Springer, Singapore (2020). https://doi.org/10.1007/978-981-32-9971-9_6

70. Deb Barma, J., Roy, J., Saha, S.C., Roy, B.S.: Process parametric optimization of submerged arc welding by using utility based Taguchi concept. Adv. Mater. Res. **488–489**, 1194–1198 (2012). https://doi.org/10.4028/www.scientific.net/AMR.488-489.1194

71. Vommi, V.B.: Topsis with statistical distances: A new approach to MADM. Decis. Sci. Lett. **6**, 49–66 (2017). https://doi.org/10.5267/j.dsl.2016.8.001

72. Panda, S.N., Bagal, D.K., Pattanaik, A., kumar, Patnaik, D., Barua, A., Jeet, S., Parida, B., Naik, B.: Comparative Evaluation for Studying the Parametric Influences on Quality of Electrode Using Taguchi Method Coupled with MOORA, DFA, and TOPSIS Method for Electrochemical Machining. In: Recent Advances in Mechanical Infrastructure. pp. 115–129 (2020). https://doi.org/10.1007/978-981-32-9971-9_13

73. Sonkar, V., Abhishek, K., Datta, S., Mahapatra, S.S.: Multi-objective Optimization in Drilling of GFRP Composites: A Degree of Similarity Approach. In: 3rd International Conference on Materials Processing and Characterisation (ICMPC 2014). pp. 538–543. Elsevier BV (2014). https://doi.org/10.1016/j.mspro.2014.07.068

74. Kamaraj, M., Santhanakrishnan, R., Muthu, E.: Investigation of surface roughness and MRR in drilling of Al2O3 particle and sisal fibre reinforced epoxy composites using TOPSIS based Taguchi method. In: IOP Conference Series: Materials Science and Engineering. Institute of Physics Publishing (2018). https://doi.org/10.1088/1757-899X/402/1/012095

75. Dinbandhu, Abhishek, K.: Parametric Optimization and evaluation of RMD^{TM} Welding performance for ASTM A387 Grade 11 Steel plates using TOPSIS-Taguchi Approach. In: Advances in Materials Processing and Manufacturing Applications. iCADMA 2020. Lecture Notes in Mechanical Engineering, pp. 215–227. Springer, Singapore (2021). https://doi.org/10.1007/978-981-16-0909-1_22

76. Sun, C.C., Lin, G.T.R.: Using fuzzy TOPSIS method for evaluating the competitive advantages of shopping websites. Expert Syst. Appl. **36**, 11764–11771 (2009). https://doi.org/10.1016/j.eswa.2009.04.017

77. Velasquez, M., Hester, P.T.: An Analysis of Multi-Criteria Decision Making Methods. (2013)